REFERENCES AND NOTES

1. J. E. Sulston and H. R. Horvitz, *Dev. Biol.* **56**, 110 (1977); J. E. Kimble and D. Hirsh, *ibid.* **70**, 396 (1979); J. E. Sulston, E. Schierenberg, J. G. White, J. N. Thomas, *ibid.* **100**, 64 (1983); I. S. Greenwald, P. W. Sternberg, H. R. Horvitz, *Cell* **34**, 435 (1983); E. M. Hedgecock, *Trends Neurosci.* **8**, 288 (1985).
2. D. A. Weisblat, R. T. Sawyer, G. S. Stent, *Science* **202**, 1295 (1978); H. Balakier and R. A. Pedersen, *Dev. Biol.* **90**, 352 (1982); C. Holt, T. W. Bertsch, H. M. Ellis, W. A. Harris, *Neuron* **1**, 15 (1988).
3. D. A. Weisblat, S. L. Zackson, S. S. Blair, J. D. Young, *Science* **209**, 1538 (1980); R. L. Gimlich and J. Braun, *Dev. Biol.* **109**, 509 (1985); M. Bronner-Fraser and S. E. Fraser, *Nature* **335**, 161 (1988); R. Wetts and S. E. Fraser, *Science* **239**, 1142 (1988).
4. J. Price, D. Turner, C. Cepko, *Proc. Natl. Acad. Sci. U.S.A.* **84**, 156 (1987); J. R. Sanes, J. L. R. Rubenstein, J.-F. Nicolas, *EMBO J.* **5**, 3133 (1986); D. L. Turner and C. L. Cepko, *Nature* **328**, 131 (1987).
5. Zebrafish: C. B. Kimmel and R. M. Warga, *Science* **231**, 365 (1986); sea urchin: R. A. Cameron, S. E. Fraser, R. J. Britten, E. H. Davidson, *Genes Dev.* **1**, 75 (1987).
6. P. A. Wilson, G. Oster, R. Keller, *Development* **105**, 155 (1989); R. M. Akers, C. R. Phillips, N. K. Wessels, *Science* **231**, 613 (1986); R. Keller, J. Shih, P. Wilson, *Gastrulation: Movements, Patterns, and Molecules*, R. Keller, W. Clark, and F. Griffen, Eds. (Plenum, New York, 1991).
7. M. K. Stehling, R. Turner, P. Mansfield, *Science* **254**, 43 (1991); P. G. Morris, *Nuclear Magnetic Resonance Imaging in Biology & Medicine* (Oxford Univ. Press, New York, 1986); P. Mansfield and P. G. Morris, *NMR Imaging in Biomedicine* (Academic Press, New York, 1982).
8. C. T. W. Moonen, P. C. M. van Zijl, J. A. Frank, D. Le Bihan, E. D. Becker, *Science* **250**, 53 (1990).
9. We use the steady-state free precession technique with a short repetition time (150 ms) so that the signal is observed preferentially from those spins that return to equilibrium most rapidly (short T_1) (*7, 23*). A short echo time (4.5 ms) is used to minimize T_2 effects.
10. D. H. Lee, *J. Can. Assoc. Radiol.* **42**, 6 (1991).
11. S. C. Wang *et al.*, *Radiology* **175**, 483 (1990); W. A. Gibby, A. Bogdan, T. W. Ovitt, *Invest. Radiol.* **24**, 302 (1989).
12. R. B. Lauffer, *Chem. Rev.* **87**, 901 (1987); G. E. Jackson, S. Wynchank, M. Woudenberg, *Magn. Reson. Med.* **16**, 57 (1990).
13. J. B. Aguayo, S. J. Blackband, J. Schoeniger, M. A. Mattingly, M. Hintermann, *Nature* **322**, 190 (1988); G. A. Johnson, M. B. Thompson, S. L. Gewalt, C. E. Hayes, *J. Magn. Reson.* **68**, 129 (1986); R. W. Behling, H. K. Tubbs, M. D. Cockman, L. W. Jelinski, *Nature* **341**, 321 (1989); C. F. Jenner, Y. Xai, C. D. Eccles, P. T. Calllaghan, *ibid.* **336**, 399 (1988).
14. W. Kuhn, *Angew. Chem. Int. Ed. Engl.* **29**, 1 (1990); P. T. Callaghan and C. D. Eccles, *J. Magn. Reson.* **78**, 1 (1988); P. Glover *et al.*, *Proceedings of the Society of Magnetic Resonance in Medicine, 8th Annual Meeting*, Amsterdam, 12 to 18 August 1989 (Society of Magnetic Resonance in Medicine, Berkeley, CA, 1989), p. 285. X. Zhou *et al.*, *ibid.*, p. 286.
15. Z. H. Cho *et al.*, *Med. Phys.* **15**, 815 (1988).
16. R. Wetts and S. E. Fraser, *Development* **105**, 9 (1989); S. Moody, *Dev. Biol.* **119**, 560 (1987); L. Dale and J. M. W. Slack, *Development* **99**, 527 (1987). Blastomere DA gives rise to head epidermis; retina; lens; portions of the prosencephalon, mesencephalon, and rhombencephalon; and spinal cord.
17. The relative size of the MRI label–excluded region is appropriate to the size of nuclei at this stage [W. W. Mathews, *Atlas of Descriptive Embryology* (Macmillan, New York, 1986)], and we have observed that the analogous rhodamine label is excluded from nuclei.
18. G. W. Eagleson and W. A. Harris, *J. Neurobiol.* **21**, 427 (1990).
19. R. E. Keller, M. Danilichik, R. Gimlich, J. Shih, in *Molecular Biology*, vol. 31 of *New Series*, G. M. Edelman, Ed. (Liss, New York, 1985). The intercalation of deep cells has been observed by Keller and co-workers by grafting tissue with fluorescently labeled cells into unlabeled embryos.
20. J. M. W. Slack and D. Tannahill, *Development* **114**, 285 (1992).
21. E. L. Effmann, G. A. Johnson, B. R. Smith, G. A. Talbott, G. Cofer, *Teratology* **38**, 59 (1988).
22. W. E. Conner, G. A. Johnson, G. P. Cofer, K. Dittrich *et al.*, *Experientia* **44**, 11 (1988).
23. C. D. Eccles and P. T. Callaghan, *J. Magn. Reson.* **68**, 393 (1986); C. B. Ahn and Z. H. Cho, *Med. Phys.* **16**, 22 (1989); J. H. Maki, G. A. Johnson, G. P. Cofer, J. R. MacFall, *J. Magn. Reson.* **80**, 482 (1988); P. T. Callaghan, *Principles of Nuclear Magnetic Resonance Microscopy* (Oxford Univ. Press, New York, 1991).
24. A single blastomere was pressure-injected with ~20 nl of a solution of Gd-DTPA-dextran (100 mg/ml, 17 kD average molecular mass). Embryos were sealed in a 2.5-mm outer diameter glass NMR tube in 10% Ringer solution and maintained at 17°C. A 1% solution of low-temperature gelling agar in rearing solution was used for later stage embryos to minimize movement. The MRI procedure had no obvious adverse effects on the development of the embryos. A 3D spin echo-pulse sequence with a 150-ms recycle time, 4.5-ms echo time, 10-μs dwell time, and 256 by 256 by (32 or 64) data array was used. The time to record a full 3D data set was 90 min. The slice direction data were zero-filled before the 3D Fourier transform to achieve isotropic resolution. Given the strength of the magnetic field gradients used (75 G/cm), this data collection scheme yielded an in-plane pixel resolution of 12 μm and a slice thickness of 72 or 36 μm.
25. R. E. Jacobs and S. E. Fraser, personal observation.

26. We thank Z. H. Cho, C. B. Ahn, and S. Juh for assistance in the initial phases of this project; and J. Shih, A. Collazo, and J. Ivins for comments on the manuscript. Supported by National Institutes of Health grant HD 25390, the Baxter Foundation, and a gift from the Monsanto-Searle Company.

27 August 1993; accepted 24 November 1993

Disruption of PDGF Receptor Trafficking by Mutation of Its PI-3 Kinase Binding Sites

Marguerite Joly, Andrius Kazlauskas, Fredric S. Fay, Silvia Corvera*

Human platelet-derived growth factor receptors (PDGFRs) expressed in human Hep G2 cells internalized and concentrated in a juxtanuclear region near the Golgi network within 10 minutes after the cells were treated with PDGF. A PDGFR mutant (F5) that lacks high-affinity binding sites for the Src homology 2 domain-containing proteins phosphatidylinositol-3 kinase (PI-3 kinase), Ras guanosine triphosphatase activating protein, phospholipase C–γ, and a phosphotyrosine phosphatase (Syp) remained at the cell periphery. Restoration of the PI-3 kinase binding sites on F5 completely restored the ability of the receptor to concentrate intracellularly. A PDGFR mutant lacking only PI-3 kinase binding sites failed to concentrate intracellularly. Thus, PI-3 kinase binding sites appear both necessary and sufficient for the normal endocytic trafficking of the activated PDGFR.

Activation of receptor tyrosine kinases initiates intracellular signaling pathways that regulate cellular growth and development (*1*). Activated receptors rapidly internalize, leading to the degradation of the ligand, the receptor, or both (*2*). Internalization of receptor tyrosine kinases is likely to be an important mechanism for securing tight control of cellular growth and proliferation. Important differences exist between the internalization of receptor tyrosine kinases and that of receptors for macromolecular nutrients such as low density lipoproteins and transferrin. The latter internalize and recycle constitutively, but receptor tyrosine kinases internalize only when activated by ligand (*2*). Ligand binding induces autophosphorylation on tyrosines of the receptor cytoplasmic domain and its association with signaling proteins that contain Src homology 2 domains. These include phospholipase C–γ (PLC-γ), the guanosine triphosphatase activating protein for Ras (GAP), the 65-kD phosphotyrosine phosphatase (Syp), nonreceptor tyrosine kinases (*3*), and PI-3 kinase (*4*). This enzyme catalyzes the phosphorylation of phosphatidylinositol (PIns), PIns(4)P, and PIns(4,5)P_2 at the 3′ position of the inositol ring, but the biological functions of these lipids are not known.

We tested the hypothesis that the trafficking of receptor tyrosine kinases is driven by the regulatory proteins that are recruited to the autophosphorylated cytoplasmic domain. The activated PDGFR binds to a large number of regulatory proteins (*5*) and is rapidly internalized and degraded (*6*). The role of regulatory proteins in the internalization and trafficking of the human β-PDGFR was analyzed in cells expressing

M. Joly and S. Corvera, Program in Molecular Medicine and Department of Cell Biology, University of Massachusetts Medical School, 373 Plantation Street, Worcester, MA 01605.
A. Kazlauskas, National Jewish Hospital for Immunology and Respiratory Medicine, Denver, CO 80206.
F. S. Fay, Program in Molecular Medicine and Biomedical Imaging Group, University of Massachusetts Medical School, Worcester, MA 01655.

*To whom correspondence should be addressed.

mutant receptors that lack high-affinity binding sites for regulatory proteins (*7*). The F5 mutant is a receptor in which Tyr^{740}, Tyr^{751}, Tyr^{771}, Tyr^{1009}, and Tyr^{1021} are substituted with phenylalanine and is deficient in the binding of PI-3 kinase, PLC-γ, GAP, and Syp (*8*). A receptor restored in the high-affinity binding of PI-3 kinase ($Tyr^{40,51}$) was generated by mutation of Phe^{740} and Phe^{751} in F5 back to tyrosine. A receptor exclusively deficient in the binding of PI-3 kinase ($Phe^{40,51}$) was constructed by substituting Tyr^{740} and Tyr^{751} with phenylalanine (*9*). Each construct was introduced into human Hep G2 cells, which do not express endogenous β-PDGFRs, with the pLXSN retroviral expression vector (*8*). All constructs were expressed at approximately 5×10^5 receptors per cell (*8*) and were activated by ligand (*10*) (Fig. 1).

To monitor the intracellular trafficking of the receptor, we used a monoclonal antibody that binds to the exofacial domain of the human β-PDGFR but does not block the activation of the receptor by PDGF and does not induce receptor down-regulation (Fig. 2) (*11*, *12*). A punctate uniform pattern of fluorescence was observed on the plasma membrane of cells held at 5°C (Fig. 2). Upon incubation for 10 min at 37°C, the antibody appeared to internalize and concentrate in a juxtanuclear region (Fig. 2). Juxtanuclear concentration of the antibody was not observed in cells that expressed the F5 mutant receptor, which appeared to remain at the cell periphery (Fig. 2). Restoration of the PI-3 kinase binding sites restored the concentration of the receptor in the juxtanuclear region (Fig. 2). To determine whether binding sites other than those for PI-3 kinase can also modulate receptor trafficking, we analyzed the cellular localization of receptors deficient only in high-affinity binding sites for PI-3 kinase. The staining pattern observed with this mutant resembled that observed with F5 (Fig. 2).

To localize the juxtanuclear region in which the antibody concentrated, we double stained cells with *Lens culinaris* lectin (*12*), which marks internal secretory compartments, predominantly the Golgi apparatus. To improve image resolution, we analyzed individual cells by optical sectioning and image reconstruction (*13*). Wild-type or $Tyr^{40,51}$ mutant receptors concentrated in the region of maximal lectin staining, but the staining patterns were distinctly different (Fig. 3). In cells expressing the F5 or $Phe^{40,51}$ mutants, no antibody was found concentrated in this region. Thus, tyrosine phosphorylation of residues 740 and 751 appears to be both necessary and sufficient to target the activated receptor from the plasma membrane to a compartment close to the Golgi apparatus.

To address the possibility that the observed targeting of the PDGFR might be artificially induced by the antibody to the exofacial domain, we treated cells with PDGF only and fixed and stained them with a PDGFR polyclonal antibody to the cytoplasmic domain (Fig. 4). The signal was

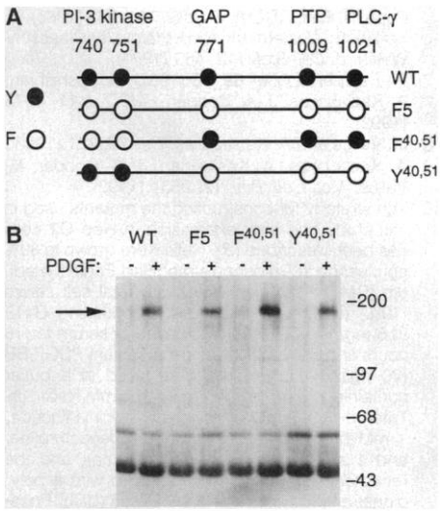

Fig. 1. Mutant constructs of the PDGFR. (**A**) Closed circles represent the tyrosine (Y) residues in the human β-PDGFR cytoplasmic domain. The proteins that bind to these sites are indicated above the residue number. Open circles represent tyrosine to phenylalanine (F) substitutions. WT, wild type; PTP, protein tyrosine phosphatase. (**B**) PDGFRs were immunoprecipitated from cells treated with buffer (−) or PDGF (+) (20 ng/ml) for 10 min at 37°C and immunoblotted with a monoclonal antibody to phosphotyrosine. The arrow indicates the expected molecular size of the receptor. Molecular size markers are indicated to the right in kilodaltons.

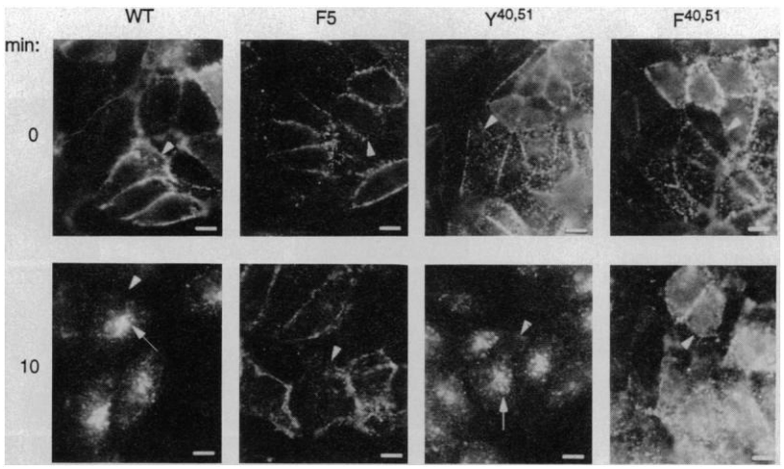

Fig. 2. Internalization of antibody to the PDGFR. Cells that expressed various receptors (indicated at the top) were incubated simultaneously with PDGF (20 ng/ml) and monoclonal antibody to the PDGFR (5 μg/ml) for 70 min at 5°C, washed with DMEM at 5°C, and then incubated for 10 min at 5°C to prevent endocytosis (top panels, 0 min of internalization) or at 37°C to allow endocytosis (lower panels, 10 min of internalization). Antibody was visualized with goat antibodies to mouse IgG coupled to rhodamine. Arrowheads indicate the boundary of randomly selected cells. Arrows indicate the region where the wild-type and $Tyr^{40,51}$ receptors concentrate. Bars, 10 μm.

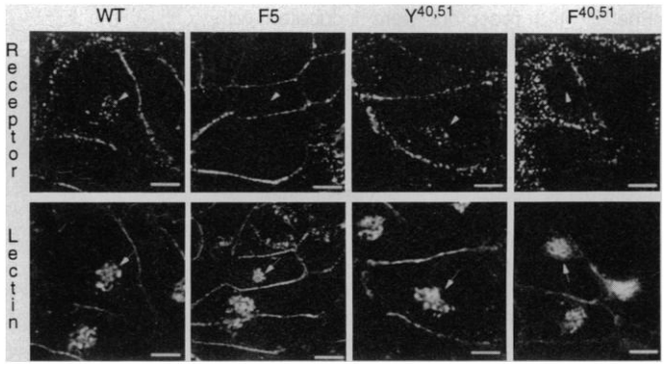

Fig. 3. Simultaneous detection of antibody to the PDGFR and compartments containing *N*-acetylglucosamine. After 10 min of antibody internalization, cells were fixed and stained with goat antibodies to mouse IgG coupled to rhodamine and with *Lens culinaris* lectin coupled to FITC. Twenty-five serial two-dimensional images were recorded at 0.25-μm intervals with a charged-coupled device camera (Photometrics). The blurring of fluorescence from regions above and below the plane of focus was reversed (*13*). Shown is the sum of 10 optical sections that contained the maximal lectin fluorescence intensity (arrows). The corresponding region in the rhodamine images is shown in the upper panels (arrowheads). Bars, 10 μm.

diffusely distributed on the plasma membrane of cells maintained at 5°C (Fig. 4) but was concentrated in the juxtanuclear region of cells that expressed wild-type or $Tyr^{40,51}$ mutant receptors after 10 and 20 min of warming. These results indicate that the juxtanuclear concentration of receptors was not induced by the exofacial domain antibody.

To determine the degree to which receptor mutants progressed in the endocytic pathway, we measured the amount of bound antibody remaining accessible to the extracellular space after 10 min of internalization. Approximately 75% of bound antibody was released by acid washing from cells expressing the F5 and $Phe^{40,51}$ mutant receptors, and approximately 30% was released from cells expressing the wild-type receptor or the $Tyr^{40,51}$ mutant. Thus, the lack of PI-3 kinase binding sites appears to affect receptor trafficking in the early steps of the endocytic pathway (*14*).

The failure of the receptors to progress through the endocytic pathway was also reflected by a decrease in the rate of PDGF-induced receptor degradation of the F5 and $Phe^{40,51}$ mutants. The restoration of PI-3 kinase binding sites restored rapid PDGF-induced degradation (Fig. 5). It has recently been shown that one of the PI-3 kinase binding sites, Tyr^{751}, can also bind the SH2-SH3–containing protein Nck (*15*). The extent of Nck binding to the receptor in vivo, relative to PI-3 kinase, is not known, but it is possible that receptor trafficking may be influenced by PI-3 kinase, Nck, or both.

The cloning of the catalytic subunit of PI-3 kinase revealed an unexpected similarity to a yeast protein, Vps34p (*16*), which plays a critical role in the delivery of newly synthesized proteins to the yeast vacuole (*17*). The high degree of similarity between Vps34p and PI-3 kinase suggests that both enzymes could fulfill similar functions. We propose that PI-3 kinase mediates growth factor receptor trafficking in the endocytic pathway and that the sorting function of this enzyme has been conserved from yeast to mammals.

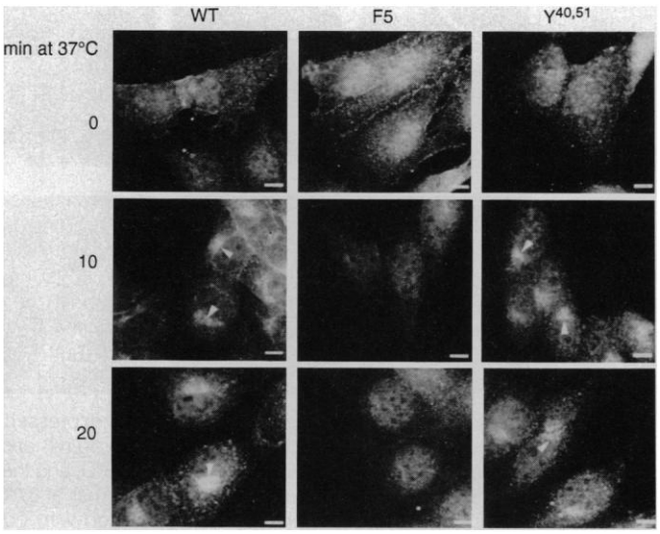

Fig. 4. Immunofluorescence analysis of PDGFRs. Cells were incubated with PDGF (20 ng/ml) for 70 min at 5°C, washed, incubated at 37°C for the time indicated on the left, fixed, and stained with a polyclonal antibody to the cytoplasmic domain of the PDGFR and goat antibodies to rabbit IgG coupled to FITC. Arrowheads point to the region of concentration of the wild-type and $Tyr^{40,51}$ receptors. Bars, 10 μm.

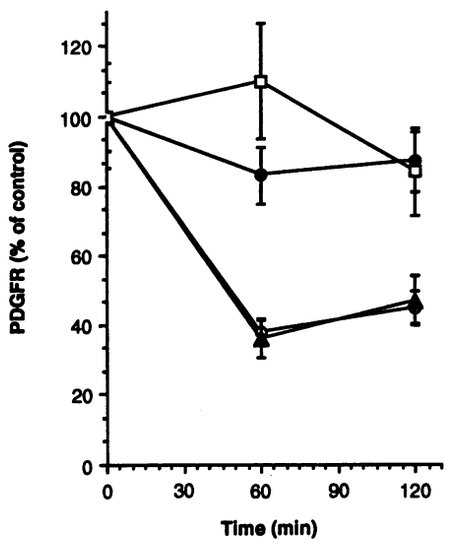

Fig. 5. Degradation of PDGFRs. Cells expressing the wild-type (○), F5 (●), $Tyr^{40,51}$ (▲), or $Phe^{40,51}$ (□) receptors were incubated with methionine-free DMEM containing [^{35}S]methionine (100 μCi/ml; Amersham) for 3 hours and then for 30 min in DMEM containing bovine serum albumin (1%) and methionine (0.3 mg/ml). Cells were then incubated without or with PDGF (30 ng/ml) for the times indicated. Fluorograms of receptor immunoprecipitates resolved by SDS–polyacrylamide gel electrophoresis were scanned with a laser densitometer. The intensity of the mature receptor (190 kD) from PDGF-treated cells was expressed as the percent of the intensity of the receptor from corresponding nontreated cells. All receptor constructs had a half-life of approximately 3 hours in the absence of PDGF. Each point represents the mean of four (wild-type, F5, and $Tyr^{40,51}$) or two ($Phe^{40,51}$) independent experiments.

REFERENCES AND NOTES

1. L. C. Cantley *et al.*, *Cell* **64**, 281 (1991).
2. H. Haigler, J. F. Ash, S. J. Singer, S. Cohen, *Proc. Natl. Acad. Sci. U.S.A.* **75**, 3317 (1978); J. Schlessinger, Y. Schechter, M. C. Willingham, I. Pastan, *ibid.*, p. 2659; P. Gorden, J. L. Carpentier, P. Freychet, A. LeCam, L. Orci, *Science* **200**, 782 (1978); C. M. Stoscheck and G. Carpenter, *J. Cell. Physiol.* **120**, 296 (1984); S. Marshall and G. Olefsky, *Endocrinology* **107**, 1937 (1980); J. M. Backer, C. R. Kahn, M. F. White, *J. Biol. Chem.* **264**, 1694 (1989); J. Goldstein, M. S. Brown, R. G. W. Anderson, D. W. Russell, W. J. Schneider, *Annu. Rev. Cell Biol.* **1**, 1 (1985).
3. A. Ullrich and J. Schlessinger, *Cell* **61**, 203 (1990); D. A. Kumijan, M. I. Wahl, S. G. Rhree, T. O. Daniel, *Proc. Natl. Acad. Sci. U.S.A.* **86**, 8232 (1989); M. F. Moran, P. Polakis, F. McCormick, T. Pawson, C. Ellis, *Mol. Cell. Biol.* **11**, 1804 (1991); F. Gen-Sheng, H. Chi-Chung, T. Pawson, *Science* **259**, 1607 (1993); W. Vogel, R. Lammers, J. Huang, A. Ullrich, *ibid.*, p. 1611; R. M. Kypta, Y. Goldberg, E. T. Ulug, S. A. Courtneidge, *Cell* **62**, 481 (1990).
4. K. R. Auger, L. A. Serunian, S. P. Soltoff, P. Libby, L. C. Cantley, *Cell* **57**, 167 (1989); S. R. Coughlin, J. A. Escobedo, L. T. Williams, *Science* **243**, 1191 (1989); M. Otsu *et al.*, *Cell* **65**, 91 (1991); I. D. Hiles *et al.*, *ibid.* **70**, 419 (1992).
5. M. Pazin and L. Williams, *Trends Biochem. Sci.* **17**, 374 (1992).
6. J. Nilsson, J. Thyberg, C. H. Heldin, B. Westermark, A. Wasteson, *Proc. Natl. Acad. Sci. U.S.A.* **80**, 5592 (1983); M. E. Rosenfeld, D. Bowen-Pope, R. Ross, *J. Cell. Physiol.* **121**, 263 (1985); A. Sorkin, B. Westermark, C. H. Heldin, L. Claesson-Welsh, *J. Cell Biol.* **112**, 469 (1991).
7. W. Fantl *et al.*, *Cell* **69**, 13 (1992); A. Kashishian, A. Kazlauskas, J. A. Cooper, *EMBO J.* **11**, 1373 (1992).
8. M. Valius and A. Kazlauskas, *Cell* **73**, 321 (1993).
9. A. Kazlauskas, A. Kashishian, J. A. Cooper, M. Valius, *Mol. Cell. Biol.* **12**, 2534 (1992).
10. The strategy for constructing the mutants used in this study and their expression in Hep G2 cells has been described (*8*). Cells were grown to 80% confluence in Dulbecco's modified Eagle's medium (DMEM) supplemented with fetal calf serum (10%) (UBI, Lake Placid, NY) containing G418 (0.5 mg/ml). Cells were deprived of serum for 18 hours and stimulated with recombinant PDGF-BB (20 ng/ml) (UBI). Cells were lysed in a buffer containing 20 mM tris (pH 8.0), 150 mM NaCl, 1% Triton X-100, 2 mM phenylmethylsulfonyl fluoride, 1 mM benzamidine, 1 mM 1,10-phenanthroline, and 1 mM sodium vanadate (Sigma), and the receptors were immunoprecipitated with a polyclonal antibody to α- and β-PDGFR (UBI). Phosphotyrosine antibody 4G10 (UBI) was used for immunoblotting.
11. L. Ronnstrand *et al.*, *J. Biol. Chem.* **263**, 10429 (1988).
12. Cells were grown to 85% confluence on glass cover slips, serum-deprived for 24 hours, and incubated for 70 min with both PDGF (20 ng/ml) and monoclonal antibody PDGFR-B2 (5 μg/ml) (Oncogene Sciences) at 5°C. Cells were fixed by immersion in methanol at −20°C for 6 min. Antibody to the receptor was detected with goat antibodies to mouse immunoglobulin G (IgG) coupled to rhodamine or fluorescein isothiocyanate (FITC) (Tago). Cellular compartments containing terminal *N*-acetylglucosamine were stained with FITC-coupled *Lens culinaris* lectin (5 μg/ml) (E-Y Laboratories, San Mateo, CA).
13. Data were processed and visualized on a Silicon

Graphics 4D/240 GTX as described [W. Carrington, K. E. Fogarty, F. S. Fay, in *Non-Invasive Techniques in Cell Biology*, K. Foster, Ed. (Wiley-Liss, New York, 1990), pp. 53–72]. This software is now available for a personal computer from Scanalytics (Billerica, MA).
14. S. L. Schmid and E. Smythe, *J. Cell Biol.* 114, 869 (1991).
15. R. Nishimura *et al.*, *Mol. Cell. Biol.* 13, 6889 (1993).
16. J. H. Stack, P. K. Herman, P. V. Schu, S. D. Emr, *EMBO J.* 12, 2195 (1993); P. V. Schu *et al.*, *Science* 260, 88 (1993).
17. D. J. Klionsky, P. K. Herman, S. D. Emr, *Microb. Rev.* 54, 266 (1990).
18. We thank D. Bowman and E. Moore for help with image analysis and M. Czech for comments on the manuscript. Supported by grants to S.C. (NIH-DK40330), F.S.F. (NSF-BIR9200027), and A.K. (NIH-GM48339).

17 August 1993; accepted 13 December 1993

Nitric Oxide Activation of Poly(ADP-Ribose) Synthetase in Neurotoxicity

Jie Zhang, Valina L. Dawson, Ted M. Dawson, Solomon H. Snyder*

Poly(adenosine 5′-diphosphoribose) synthetase (PARS) is a nuclear enzyme which, when activated by DNA strand breaks, adds up to 100 adenosine 5′-diphosphoribose (ADP-ribose) units to nuclear proteins such as histones and PARS itself. This activation can lead to cell death through depletion of β-nicotinamide adenine dinucleotide (the source of ADP-ribose) and adenosine triphosphate. Nitric oxide (NO) stimulated ADP-ribosylation of PARS in rat brain. Benzamide and other derivatives, which inhibit PARS, blocked *N*-methyl-D-aspartate– and NO-mediated neurotoxicity with relative potencies paralleling their ability to inhibit PARS. Thus, NO appeared to elicit neurotoxicity by activating PARS.

Nitric oxide is a messenger molecule that regulates macrophage killing of tumor cells and bacteria (*1*) and blood vessel relaxation (*2*) and also is a neurotransmitter (*3*). When produced in large quantities in response to actions of the excitatory neurotransmitter glutamate acting at *N*-methyl-D-aspartate (NMDA) receptors, NO mediates neuronal killing (*4, 5*). Toxicity due to NMDA may account for neural damage in vascular stroke, as NO synthase (NOS) inhibitors prevent stroke damage (*6*). Mechanisms proposed for NO neurotoxicity as well as tumoricidal and bactericidal actions include monoADP-ribosylation and S-nitrosylation of glyceraldehyde-3-phosphate dehydrogenase (GAPDH) (*7*), inhibition of mitochondrial enzymes such as *cis*-aconitase (*8*), inhibition of the mitochondrial electron transport chain (*1*), inhibition of ribonucleotide reductase (*9*), and DNA damage (*10, 11*). DNA damage activates PARS (E.C. 2.4.2.30) (*12, 13*). Here we show that NO activates PARS in association with damage to DNA, and that PARS inhibitors prevent NMDA neurotoxicity with relative potencies paralleling their inhibition of the enzyme.

In rat brain nuclear extracts, PARS activity was almost tripled in a dosage-dependent manner when DNA that had been preincubated with NO was added (Fig. 1A) (*14*). Addition of covalently closed circular DNA by itself had no effect on PARS activity. Both 4-amino-1,8-naphthalimide and 1,5-dihydroxyisoquinoline, two potent PARS inhibitors, reduced the activity to <5% of basal levels (Fig. 1A). The major protein ADP-ribosylated in the nuclear extracts was PARS itself (Fig. 1B). Similarly, DNA that had been treated with 3-morpholinosyndnonimine (SIN-1) and sodium nitroprusside (SNP), two NO donors, could stimulate poly(ADP-ribose) synthesis, which was inhibited by benzamide, another PARS inhibitor (*14*). Neither SNP nor SIN-1 alone had an effect on PARS (*14*).

McDonald and Moss have demonstrated that NO-enhanced modification of GAPDH by β-nicotinamide adenine dinucleotide (NAD) involves the transfer of the entire NAD to a thiol group rather than ADP-ribosylation (*7*). To ensure that the polymer formed from NAD in our study was poly(ADP-ribose), we used both [*adenine*-^{14}C]NAD and [*nicotinamide*-^{14}C]NAD and found radioactivity could only be incorporated into the polymers from the former compound (*14*).

To directly determine if PARS activation participates in NMDA neurotoxicity, we monitored neurotoxicity elicited by NMDA in rat cerebral cortical cultures in which NOS inhibitors provided protection (Fig. 2) (*4*). Increasing concentrations of NMDA progressively augmented neuronal killing. Benzamide (100 μM) provided 40 to 50% protection at all NMDA concentrations examined. At a benzamide concentration of 50 μM, there was no significant protection detected; but 500 μM benzamide provided ~30% more protection than 100 μM benzamide (Table 1). NO did not interact with benzamide (*15*). A variety of benzamide derivatives exist with differing potencies as PARS inhibitors. In the family of benzamide and its derivatives, benzamide is the most active, 3-aminobenzamide is about 50% as potent and 4-aminobenzamide is 1 to 2% as potent as benzamide, and benzoic acid is inactive (*16*). Benzamide provided the most protection against NMDA neurotoxicity and 3-aminobenzamide exerted somewhat less protection, but 4-aminobenzamide and benzoic acid did not protect at all (Table 1). A structurally unrelated PARS inhibitor, 1,5-dihydroxyisoquinoline (10 μM), was also neuropro-

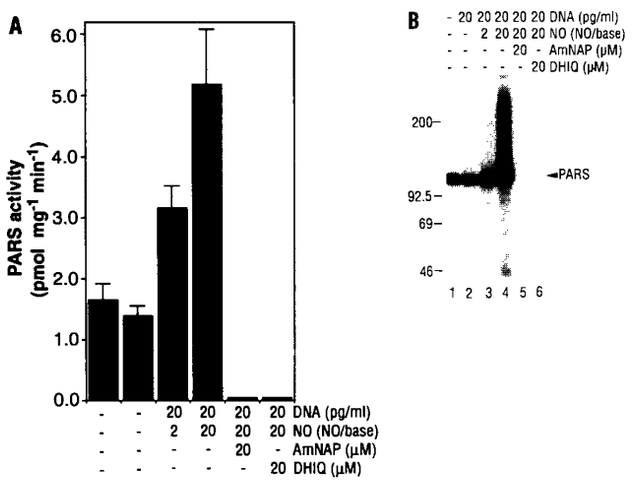

Fig. 1. Activation of PARS by NO-damaged DNA. (**A**) PARS activity after different treatments (mean ± SEM, n = 3) (*14*). (**B**) Autoradiography of poly-ADP-ribosylation of PARS on 7.5% SDS–polyacrylamide gel electrophoresis. Sizes are indicated at left in kilodaltons. Abbreviations: AmNAP, 4-amino-1,8-naphthalimide; DHIQ, 1,5-dihydroxyisoquinoline.

J. Zhang, Department of Neuroscience, Johns Hopkins University School of Medicine, Baltimore, MD 21205.
V. L. Dawson, National Institute on Drug Abuse, Addiction Research Center, Molecular Neuropsychiatry Section, National Institutes of Health, Post Office Box 5180, Baltimore, MD 21224.
T. M. Dawson, Departments of Neuroscience and Neurology, Johns Hopkins University School of Medicine, Baltimore, MD 21205.
S. H. Snyder, Departments of Neuroscience, Pharmacology and Molecular Sciences, and Psychiatry and Behavioral Sciences, Johns Hopkins University School of Medicine, Baltimore, MD 21205.
*To whom correspondence should be addressed.